Measurement of CP observables in B 0 → DK ∗0 with D →K + K −

627 authors, including:

Bernardo Adeva
University of Santiago de Compostela

1,607 PUBLICATIONS   **35,989** CITATIONS

A. Affolder
University of Liverpool

1,503 PUBLICATIONS   **39,220** CITATIONS

Some of the authors of this publication are also working on these related projects:

E-beam water purification Uganda View project

Structural reliability View project

Measurement of CP observables in $B^0 \to DK^{*0}$ with $D \to K^+K^-$

The LHCb collaboration

E-mail: stefania.ricciardi@stfc.ac.uk

ABSTRACT: The decay $B^0 \to DK^{*0}$ and the charge conjugate mode are studied using $1.0\,\text{fb}^{-1}$ of pp collision data collected by the LHCb experiment at $\sqrt{s} = 7\,\text{TeV}$ in 2011. The CP asymmetry between the $B^0 \to DK^{*0}$ and the $\bar{B}^0 \to D\bar{K}^{*0}$ decay rates, with the neutral D meson in the CP-even final state K^+K^-, is found to be

$$\mathcal{A}_d^{KK} = -0.45 \pm 0.23 \pm 0.02,$$

where the first uncertainty is statistical and the second is systematic. In addition, favoured $B^0 \to DK^{*0}$ decays are reconstructed with the D meson in the non-CP eigenstate $K^+\pi^-$. The ratio of the B-flavour averaged decay rates in D decays to CP and non-CP eigenstates is measured to be

$$\mathcal{R}_d^{KK} = 1.36\,^{+\,0.37}_{-\,0.32} \pm 0.07,$$

where the ratio of the branching fractions of $D^0 \to K^-\pi^+$ to $D^0 \to K^+K^-$ decays is included as multiplicative factor. The CP asymmetries measured with two control channels, the favoured $B^0 \to DK^{*0}$ decay with $D \to K^+\pi^-$ and the $\bar{B}_s^0 \to DK^{*0}$ decay with $D \to K^+K^-$, are also reported.

Contents

1 Introduction

Direct CP violation can arise in $B^0 \to DK^{*0}$ decays[1] from the interference between two colour-suppressed transitions: $\bar{b} \to \bar{c}$ (Cabibbo favoured) and $\bar{b} \to \bar{u}$ (Cabibbo suppressed). The corresponding Feynman diagrams are shown in figure 1; interference occurs if the D^0 and $\overline{D}^0$ mesons decay to a common final state. The magnitude of the CP-violating asymmetry that arises from this interference is related to the value of the phase $\gamma = \arg\left[-(V_{ud}V_{ub}^*)/(V_{cd}V_{cb}^*)\right]$, the least-well determined angle of the Unitarity Triangle. A method to determine γ from hadronic B-decay rates was originally proposed by Gronau, London and Wyler (GLW) in ref. [1, 2] for various charged and neutral $B \to DK$ decay modes and can be applied to the decay mode $B^0 \to DK^{*0}$. In this mode, the charge of the kaon from the $K^{*0} \to K^+\pi^-$ decay unambiguously tags the flavour of the decaying B meson [3], hence no time-dependent tagged analysis is required.

The use of these neutral B decays is particularly interesting because the magnitude of the ratio of the suppressed over the favoured amplitude, which controls the size of the interference, is expected to be relatively large (naively a factor three larger than the analogous ratio for $B^+ \to DK^+$ decays), hence the system can exhibit large CP-violating effects, depending on the D decay. Among the modes used in the GLW method, which are studied in this paper, large CP asymmetries can be expected when the D meson is reconstructed in a CP eigenstate. Contributions from B^0 decays to the non-resonant $DK^+\pi^-$ final state, which can pollute the DK^{*0} reconstructed signal candidates due to the large natural width of the K^{*0}, can be treated in a model-independent way, as shown in ref. [4]. Studies with simulated events have shown that the $B^0 \to DK^{*0}$ mode is one of the most promising channels to provide a precise measurement of γ at LHCb [5]. Results

---

[1]Here and in the following, D represents a neutral meson that is an admixture of D^0 and $\overline{D}^0$. Inclusion of charge conjugate modes is implied unless specified otherwise.
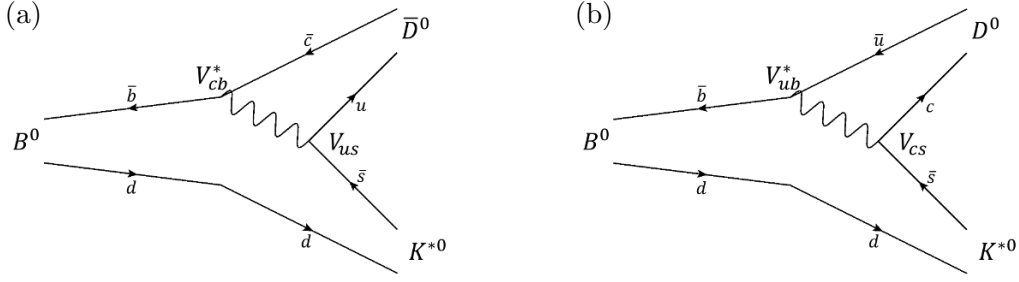
Figure 1. Feynman diagrams for (a) $B^0 \to \overline{D}^0 K^{*0}$ and (b) $B^0 \to D^0 K^{*0}$.

with this channel will therefore complement those from $B^+ \to DK^+$, which have recently been used by LHCb to constrain γ [6, 7].

This paper presents the measurement of the $B^0 - \overline{B}^0$ partial width asymmetry using D decays into the CP eigenstate K^+K^-,

$$\mathcal{A}_d^{KK} = \frac{\Gamma(\overline{B}^0 \to D_{[K^+K^-]}\overline{K}^{*0}) - \Gamma(B^0 \to D_{[K^+K^-]}K^{*0})}{\Gamma(\overline{B}^0 \to D_{[K^+K^-]}\overline{K}^{*0}) + \Gamma(B^0 \to D_{[K^+K^-]}K^{*0})}, \tag{1.1}$$

together with the measurement of the ratio of the average of the B^0 and $\overline{B}^0$ partial widths with $D \to K^+K^-$, to the average partial width with $D \to K^+\pi^-$ (where the sign of the kaon charge from the D decay is the same as that of the kaon from the K^{*0} decay),

$$\mathcal{R}_d^{KK} = \frac{\Gamma(\overline{B}^0 \to D_{[K^+K^-]}\overline{K}^{*0}) + \Gamma(B^0 \to D_{[K^+K^-]}K^{*0})}{\Gamma(\overline{B}^0 \to D_{[K^-\pi^+]}\overline{K}^{*0}) + \Gamma(B^0 \to D_{[K^+\pi^-]}K^{*0})}. \tag{1.2}$$

These quantities can be used together with other inputs to determine the value of γ. Note that the suppressed decay mode $B^0 \to D_{[K^-\pi^+]}K^{*0}$, where the sign of the kaon charge from the D decay is opposite to that of the kaon from the K^{*0} decay, is not included in this analysis. This decay mode can exhibit large CP-violating effects and can be studied with a larger dataset. The measured asymmetry in the favoured decay $B^0 \to D_{[K^+\pi^-]}K^{*0}$,

$$\mathcal{A}_d^{\mathrm{fav}} = \frac{\Gamma(\overline{B}^0 \to D_{[K^-\pi^+]}\overline{K}^{*0}) - \Gamma(B^0 \to D_{[K^+\pi^-]}K^{*0})}{\Gamma(\overline{B}^0 \to D_{[K^-\pi^+]}\overline{K}^{*0}) + \Gamma(B^0 \to D_{[K^+\pi^-]}K^{*0})} \tag{1.3}$$

is a useful cross-check since it is expected to be compatible with zero given the size of the current dataset.

In pp collisions, B_s^0 mesons are produced and can decay to the same final state, $B_s^0 \to D\overline{K}^{*0}$ [8]. In these B_s^0 decay modes, the interference between the two contributing amplitudes is expected to be small, since the relative magnitude of the suppressed to the favoured amplitude is small compared to the B^0 case. Therefore, these modes are valuable control channels, and the asymmetry

$$\mathcal{A}_s^{KK} = \frac{\Gamma(\overline{B}_s^0 \to D_{[K^+K^-]}K^{*0}) - \Gamma(B_s^0 \to D_{[K^+K^-]}\overline{K}^{*0})}{\Gamma(\overline{B}_s^0 \to D_{[K^+K^-]}K^{*0}) + \Gamma(B_s^0 \to D_{[K^+K^-]}\overline{K}^{*0})}, \tag{1.4}$$

similar to that defined in eq. (1.1), is also obtained in this analysis. Since the favoured (suppressed) $\overline{B}_s^0$ (B^0) decay gives kaons with opposite charges from D and K^{*0} decays, $\mathcal{A}_s^{\text{fav}}$ is not used as a control measurement in the analysis, to avoid biasing a potential future measurement of $\mathcal{A}_d^{\text{sup}}$.

2   The LHCb detector, dataset and event selection

The study reported here is based on a data sample collected at the Large Hadron Collider (LHC) with the LHCb detector at a centre-of-mass energy of 7 TeV during the year 2011, corresponding to an integrated luminosity of $1.0\,\text{fb}^{-1}$. The LHCb detector [9] is a single-arm forward spectrometer covering the pseudorapidity range $2 < \eta < 5$, designed for the study of particles containing b or c quarks. The detector includes a high precision tracking system consisting of a silicon-strip vertex detector surrounding the pp interaction region, a large-area silicon-strip detector located upstream of a dipole magnet with a bending power of about $4\,\text{Tm}$, and three stations of silicon-strip detectors and straw drift tubes placed downstream. The combined tracking system has a momentum resolution $\Delta p/p$ that varies from 0.4% at $5\,\text{GeV}/c$ to 0.6% at $100\,\text{GeV}/c$, and an impact parameter resolution of $20\,\mu\text{m}$ for tracks with high transverse momentum (p_T). Charged hadrons are identified using two ring-imaging Cherenkov detectors. Photon, electron and hadron candidates are identified by a calorimeter system consisting of scintillating-pad and preshower detectors, an electromagnetic calorimeter and a hadronic calorimeter. Muons are identified by a system composed of alternating layers of iron and multiwire proportional chambers. The trigger [10] consists of a hardware stage, based on information from the calorimeter and muon systems, followed by a software stage which applies a full event reconstruction.

This analysis uses events selected by the hardware level trigger either when one of the charged particles of the signal decay gives a large enough energy deposit in the calorimeter system (hadron trigger), or when one of the particles in the event, not coming from the signal decay, fulfills the trigger requirements (*i.e.* mainly events triggered by one particle coming from the decay of the other B in the event). The software trigger requires a two-, three- or four-track secondary vertex with a high scalar sum of the p_T of the tracks and a significant displacement from the primary pp interaction vertices (PVs). At least one track should have $p_\text{T} > 1.7\,\text{GeV}/c$ and an impact parameter (IP) χ^2 with respect to the PV greater than 16. The IP χ^2 is defined as the difference between the χ^2 of the PV reconstructed with and without the considered track. A multivariate algorithm is used for the identification of secondary vertices consistent with the decay of a b hadron.

Candidates are selected from combinations of charged particles. D mesons are reconstructed in the decay modes $D \to K^+\pi^-$ and K^+K^-. The p_T of the daughters is required to be larger than $400\,\text{MeV}/c$. Particle identification (PID) is used to distinguish between charged pions and kaons. The difference between the log-likelihoods of the kaon and pion hypotheses ($\text{DLL}_{K\pi}$) is required to be larger than 0 for kaons and smaller than 4 for pions. This aids the reduction of cross-feed between the signal D decay modes to a negligible level. A fit is applied to the two-track vertex, requiring that the corresponding χ^2 per degree of freedom is less than 5. In order to separate D mesons coming from a B decay from those

produced at the PV, the D candidates are required to have an IP χ^2 greater than 4 with respect to any PV. To suppress background from B decays without an intermediate D meson ($B^0 \to K^{*0}K^+K^-$ for example), for which all four charged hadrons are produced at the B-decay vertex, a condition on the D flight distance with respect to the B vertex is applied, requiring that it is larger than 0 by at least 2.5 standard deviations. Finally, D candidates with an invariant mass within $\pm 20\,\mathrm{MeV}/c^2$ of the nominal D^0 mass are retained.

K^{*0} mesons are reconstructed in the mode $K^{*0} \to K^+\pi^-$. The p_{T} of the K^+ and π^- mesons must be larger than $300\,\mathrm{MeV}/c$. PID is also used, requiring that $\mathrm{DLL}_{K\pi}$ is larger than 3 for the kaon and lower than 3 for the pion, reducing the cross-feed from $B^0 \to D\rho^0$ to a manageable level and rejecting non-resonant $B^0 \to DK^+K^-$ [11]. Possible contamination from protons in the kaon sample, $e.g.$ from $\Lambda_b^0 \to Dp\pi^-$ decays, is reduced by removing kaon candidates with a difference between the log-likelihoods of the proton and kaon hypotheses (DLL_{pK}) of less than 10. The IP χ^2 of the K^{*0} mesons must be larger than 25, to select those coming from a B decay, and their invariant mass within $\pm 50\,\mathrm{MeV}/c^2$ of the nominal mass.

$\overset{(-)}{B}{}^0_{(s)}$ meson candidates are formed by combining D and K^{*0} candidates selected with the above requirements. A fit to a common vertex is performed, keeping only combinations with χ^2 per degree of freedom lower than 4, and a kinematic fit is performed to constrain the invariant mass of the reconstructed D to the nominal D^0 mass [12]. Since B mesons are produced at the PV, only candidates with IP χ^2 lower than 9 are retained. In case several PVs are reconstructed, the one for which the B-candidate IP χ^2 is the smallest is taken as reference. Additionally, the momentum of the reconstructed B candidate is required to point back to the PV, by requiring that the angle between the B momentum direction and its direction of flight from the PV is smaller than $10\,\mathrm{mrad}$. Furthermore, the sum of the square roots of the IP χ^2 of the four charged particles must be larger than 32. The absolute value of the cosine of the K^{*0} helicity angle is required to be larger than 0.4. This angle is defined as the angle between the kaon-daughter momentum direction in the K^{*0} rest frame, and the K^{*0} direction in the B rest frame.

Specific peaking backgrounds from $B^0_{(s)} \to D^{\mp}_{(s)}h^{\pm}$ decays, where h is a π or a K meson, are eliminated by vetoing candidates for which the invariant mass of $K^+K^-\pi^+(K^-\pi^+\pi^+$ and $K^+K^-\pi^+)$ is within $\pm 15\,\mathrm{MeV}/c^2$ of the nominal mass of a D_s^+ (D^+) meson.

Where possible, data-driven methods are used to determine selection efficiencies and invariant mass distribution shapes. Otherwise, they are determined from fully simulated events. The pp collisions are generated using PYTHIA 6.4 [13] with a specific LHCb configuration [14] where, in particular, decays of hadronic particles are described by EVTGEN [15]. The interaction of the generated particles with the detector and its response are implemented using the GEANT4 toolkit [16, 17] as described in ref. [18].

3   Determination of signal yields

The numbers of reconstructed signal B^0 and B_s^0 candidates are determined from an unbinned maximum likelihood fit to their mass distributions. Candidates are split into four categories, which are fitted simultaneously: $D(K^+K^-)K^{*0}$, $D(K^+K^-)\overline{K}^{*0}$, $D(K^+\pi^-)K^{*0}$,

and $D(K^-\pi^+)\overline{K}^{*0}$. The mass distribution of each category is fitted with a sum of probability density functions (PDF) modelling the different contributing components:

1. the B^0 and B_s^0 signals are described by double Gaussian functions;

2. the combinatorial background is described by an exponential function;

3. the cross-feed from $B^0 \to D\rho^0$ decays, where one pion from the $\rho^0 \to \pi^+\pi^-$ decay is misidentified as a kaon, is described by a non-parametric PDF [19] determined from fully simulated and selected events;

4. the partially reconstructed $B^0 \to D^*K^{*0}$ and $\overline{B}_s^0 \to D^*K^{*0}$ decays, where the D^* is a D^{*0} or a $\overline{D}^{*0}$ and the π^0 or photon from the D^* decay is not reconstructed, are modelled by a non-parametric PDF determined from fully simulated and selected events.

There are 23 free parameters in the fit. These include the B^0 PDF peak position, the core Gaussian resolution for the B^0 and the B_s^0 and the slope of the combinatorial background, all of which are common to the four fit categories. The remaining free parameters are yields for each fit component within each category. Yields for $B^0_{(s)}$ and $\overline{B}^0_{(s)}$ are constrained to be identical for the background components where CP violation effects can be excluded or are expected to be compatible with zero with the current data sample size.

A separate fit to $B^0 \to D(K^+\pi^-)\rho^0$ candidates in the same data sample is performed. The yield of such candidates and the probability to reconstruct them as $B^0 \to D(K^+\pi^-)K^{*0}$ is used to constrain the number of cross-feed events in the $D(K^+\pi^-)K^{*0}$ category. The number of cross-feed candidates from $B^0 \to D(K^+K^-)\rho^0$ in the $D(K^+K^-)K^{*0}$ category is derived from the $D(K^+\pi^-)K^{*0}$ category using the relative D branching fractions and B selection efficiencies. As no flavour asymmetry is expected for this background, the numbers of cross-feed events in the $D\overline{K}^{*0}$ categories are constrained to be identical to those of the corresponding DK^{*0} categories.

The partially reconstructed background component accumulates at masses lower than the nominal B^0 mass. Its shape depends on the unknown fraction of transverse polarisation in the $\overset{(-)}{B}{}^0_{(s)} \to D^*K^{*0}$ decays. In order to model the $\overset{(-)}{B}{}^0_{(s)} \to D^*K^{*0}$ contribution, a PDF is built from a linear combination of three non-parametric functions corresponding to the three orthogonal helicity eigenstates. The functions are derived from simulated $\overset{(-)}{B}{}^0_{(s)} \to D^*K^{*0}$ events reconstructed as $B^0 \to DK^{*0}$. Each function corresponds to the weighted sum of the $D^* \to D\gamma$ and $D^* \to D\pi^0$ contributions for a defined helicity eigenstate, where the weights take into account the relative D^* decay branching fractions and the corresponding reconstruction efficiencies.

The invariant mass distributions together with the function resulting from the fit are shown in figure 2. Note that the decay $\overline{B}_s^0 \to D(K^+\pi^-)K^{*0}$ is not observed since the charge combination of the kaons in the final state corresponds to the suppressed decay. The signal yield in each category is summarized in table 1. The significance of the $B^0 \to DK^{*0}$ signal for $D \to K^+K^-$ decays, summing B^0 and $\overline{B}^0$ and including both statistical and systematic uncertainties, is found to be equal to $5.1\,\sigma$, by comparing the maximum of the likelihood of

Category	Signal yield	Category	Signal yield
$B^0 \to D_{[K^+K^-]}K^{*0}$	$21\,^{+\,6}_{-\,5}$	$\overline{B}^0 \to D_{[K^+K^-]}\overline{K}^{*0}$	8 ± 4
$B_s^0 \to D_{[K^+K^-]}\overline{K}^{*0}$	$23\,^{+\,6}_{-\,5}$	$\overline{B}_s^0 \to D_{[K^+K^-]}K^{*0}$	$24\,^{+\,6}_{-\,5}$
$B^0 \to D_{[K^+\pi^-]}K^{*0}$	$108\,^{+\,12}_{-\,11}$	$\overline{B}^0 \to D_{[K^-\pi^+]}\overline{K}^{*0}$	94 ± 11

Table 1. Signal yields with their statistical uncertainties.

the nominal fit and the maximum with the yield of the $B^0 \to D(K^+K^-)K^{*0}$ category set to zero.

The yields determined from the simultaneous mass fit are corrected for selection efficiencies in order to evaluate the asymmetries and ratios described in the introduction. The selection efficiencies account for the geometrical acceptance of the detector, the reconstruction, the PID, and the trigger efficiencies. All efficiencies are computed from fully simulated events, except for the PID and trigger efficiencies, which are obtained directly from data using clean calibration samples of $D^0 \to K^-\pi^+$ from D^{*+} decays.

4 Systematic uncertainties

Several sources of systematic uncertainty are considered, affecting either the determination of the signal yields or the computation of the efficiencies. They are summarized in table 2. In order to take into account the measured difference in the production rate between $\overline{B}^0$ and B^0, the $\overline{B}^0$ yields are multiplied by a correction factor,

$$a_{\text{prod}}^d = \frac{1 - \kappa A_{\text{prod}}}{1 + \kappa A_{\text{prod}}}, \qquad (4.1)$$

where $A_{\text{prod}} = 0.010 \pm 0.013$ [20] is the asymmetry between $\overline{B}^0$ and B^0 at production in pp collisions, and κ is a decay-dependent factor, $\kappa = \frac{\int_0^{+\infty} e^{-\Gamma t} \cos(\Delta m t)\ \epsilon(B^0 \to DK^{*0}, t)\ \mathrm{d}t}{\int_0^{+\infty} e^{-\Gamma t}\ \epsilon(B^0 \to DK^{*0}, t)\ \mathrm{d}t}$, which takes into account dilution effects due to the $B^0 - \overline{B}^0$ oscillation frequency, Δm, and includes the acceptance as a function of the decay time for the reconstructed decay, $\epsilon(B^0 \to DK^{*0}, t)$. The value of κ is found to be 0.46 ± 0.01 using fully simulated events and PID efficiencies from calibration samples. The uncertainty on a_{prod}^d is propagated to the measured observables to estimate the systematic uncertainty from the production asymmetry. Owing to the large B_s^0 oscillation frequency, the potential production asymmetry of B_s^0 mesons does not significantly affect the measurement presented here and is neglected.

The PID calibration introduces a systematic uncertainty on the calculated PID efficiencies, which propagates to the final results. All PID correction factors are compatible with unity within their uncertainties which are of the order of 1%.

The systematic uncertainty associated to the trigger is estimated by varying in the simulation the fraction of events triggered by the hadron trigger with respect to the fraction of events triggered by the other b-hadron in the event. Other selection efficiencies cancel in
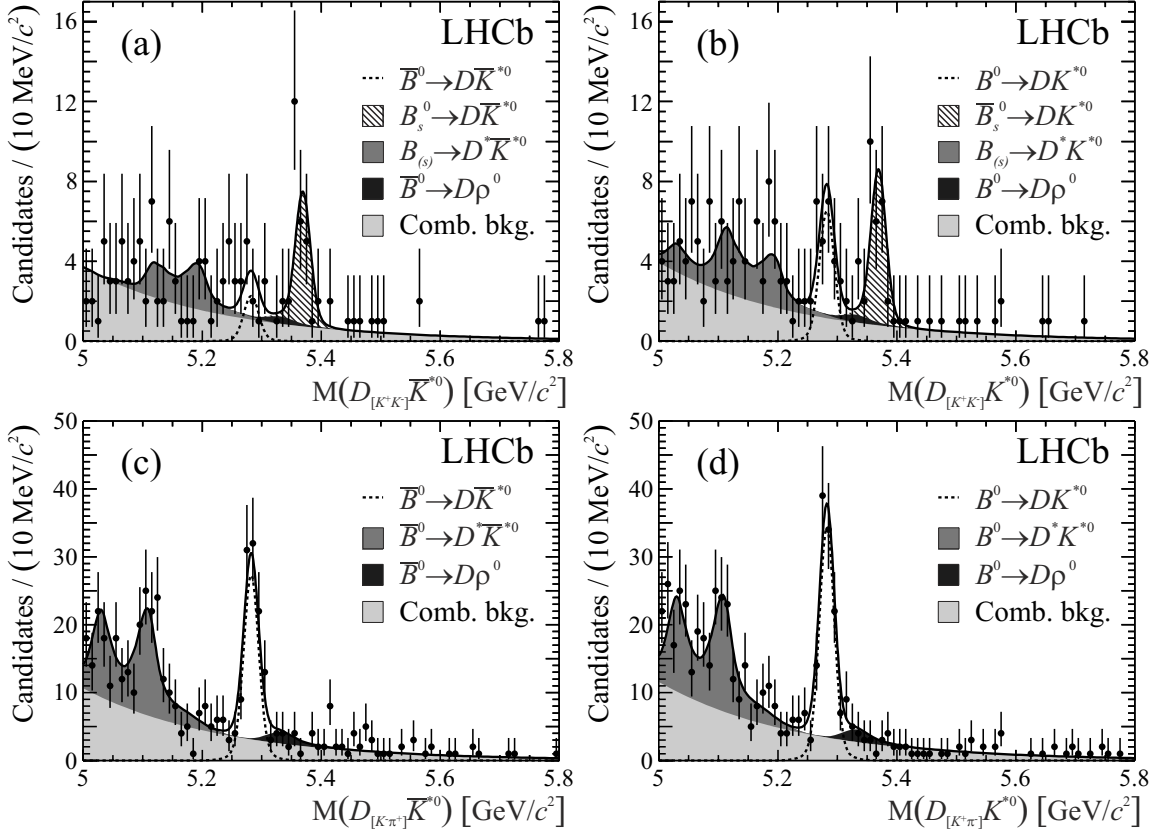
Figure 2. Invariant mass distributions of (a) $D_{[K^+K^-]}\overline{K}^{*0}$, (b) $D_{[K^+K^-]}K^{*0}$, (c) $D_{[K^-\pi^+]}\overline{K}^{*0}$ and (d) $D_{[K^+\pi^-]}K^{*0}$ candidates. The $D\overline{K}^{*0}$ distributions correspond to $\overline{B}^0$ and B_s^0 decays whereas the DK^{*0} distributions correspond to B^0 and $\overline{B}_s^0$ decays. The fit functions are superimposed; the different B decays and combinatorial background components are detailed in the legends.

the ratio of yields, except for the efficiencies of the p_T cuts on the D daughters, which are different between different D decay modes. $\mathcal{R}_d^{KK}$ has to be corrected by a multiplicative factor 0.94 ± 0.04, where the statistical uncertainty on the correction, which arises from finite simulated sample size, is assigned as systematic uncertainty due to the relative selection efficiencies.

The fit procedure is validated with simulated experiments. A bias of statistical nature, owing to the small number of events in the $B^0 \to D(K^+K^-)K^{*0}$ channel, is found to be 5% for B^0 and 8% for $\overline{B}^0$. The signal yields are corrected for this bias before computing the asymmetries and ratios. A systematic uncertainty equal to half the size of the correction has been assigned.

Simulated experiments are also used to determine the systematic uncertainties due to the low-mass background, the $B^0 \to D\rho^0$ cross-feed, and the signal shape. Samples are generated with different values of the polarisation parameters, the cross-feed fraction and the fixed signal parameters. The corresponding systematic uncertainty is estimated from the bias in the results obtained by performing the fit described in the previous section to these samples.

Source	$\mathcal{A}_d^{KK}$	$\mathcal{A}_d^{\text{fav}}$	$\mathcal{A}_s^{KK}$	$\mathcal{R}_d^{KK}$
Production asymmetry	0.005	0.006	–	0.003
PID efficiency	0.004	0.008	0.005	0.014
Trigger efficiency	0.004	0.001	0.005	0.022
Selection efficiency	–	–	–	0.040
Bias correction	0.004	–	0.001	0.013
Low-mass background	0.017	0.001	0.004	0.042
$B^0 \to D\rho^0$ cross-feed	0.001	–	0.002	0.008
Signal description	0.001	0.001	0.001	0.005
D branching fractions	–	–	–	0.022
Total	0.019	0.010	0.008	0.069

Table 2. Summary of the absolute systematic uncertainties on the measured observables.

5   Results and summary

This paper reports the analysis of $B^0 \to DK^{*0}$ decays using 1.0 fb^{-1} of pp collision data. Potential contributions to the decay amplitudes from the non-resonant $B^0 \to DK^+\pi^-$ mode are reduced by requiring that the K^{*0} reconstructed mass is within $\pm 50\,\text{MeV}/c^2$ of the nominal mass and the absolute value of the cosine of the K^{*0} helicity angle is greater than 0.4. The results for the CP-violating observables are

$$\mathcal{A}_d^{KK} = -0.45 \pm 0.23 \text{ (stat)} \pm 0.02 \text{ (syst)},$$
$$\mathcal{A}_d^{\text{fav}} = -0.08 \pm 0.08 \text{ (stat)} \pm 0.01 \text{ (syst)},$$
$$\mathcal{A}_s^{KK} = 0.04 \pm 0.16 \text{ (stat)} \pm 0.01 \text{ (syst)},$$
$$\mathcal{R}_d^{KK} = 1.36^{+\,0.37}_{-\,0.32} \text{ (stat)} \pm 0.07 \text{ (syst)}.$$

The value of $\mathcal{R}_d^{KK}$ takes into account the ratio of the branching fractions of $D^0 \to K^+K^-$ to $D^0 \to K^-\pi^+$ decays [12]. The correlation between $\mathcal{A}_d^{KK}$ and $\mathcal{R}_d^{KK}$ is equal to 0.16 and the correlations between the other observables are negligible.

These are the first measurements of CP asymmetries in B^0 and $\overline{B}_s^0$ to DK^{*0} decays with the neutral D meson decaying into a CP-even final state. Triggering, reconstructing and selecting a pure sample of these fully hadronic B decays is challenging in a high rate and high track-multiplicity environment, especially in the forward direction of LHCb. The present statistical limitations are due to a combination of several factors, the most important one being the trigger. In order to keep the output rate below its maximum of 1 MHz, the current hardware trigger imposes relatively restrictive criteria on the minimum transverse momentum of hadrons, which affect the efficiency for fully-hadronic modes. This limitation is overcome in the proposed LHCb upgrade [21, 22] by reading out the detector at the maximum LHC bunch-crossing frequency of 40 MHz. With more data, improved measurements of these and other quantities in $B^0 \to DK^{*0}$ decays will result in important constraints on the angle γ of the Unitarity Triangle.

Acknowledgments

References

[1] M. Gronau and D. London, *How to determine all the angles of the unitarity triangle from* $B_d^0 \to DK_S$ *and* $B_s^0 \to D\phi$, *Phys. Lett.* **B 253** (1991) 483 [INSPIRE].

[2] M. Gronau and D. Wyler, *On determining a weak phase from CP asymmetries in charged B decays*, *Phys. Lett.* **B 265** (1991) 172 [INSPIRE].

[3] I. Dunietz, *CP violation with selftagging* B_d *modes*, *Phys. Lett.* **B 270** (1991) 75 [INSPIRE].

[4] M. Gronau, *Improving bounds on gamma in* $B^\pm \to DK^\pm$ *and* $B^{\pm,0} \to DX_s^{\pm,0}$, *Phys. Lett.* **B 557** (2003) 198 [hep-ph/0211282] [INSPIRE].

[5] LHCb collaboration, *Roadmap for selected key measurements of LHCb*, arXiv:0912.4179 [INSPIRE].

[6] LHCb collaboration, *Observation of CP-violation in* B^+ *to* DK^+ *decays*, *Phys. Lett.* **B 712** (2012) 203 [*Erratum ibid.* **B 713** (2012) 351] [arXiv:1203.3662] [INSPIRE].

[7] LHCb collaboration, *A model-independent Dalitz plot analysis of* $B^\pm \to DK^\pm$ *with* $D \to K_S^0 h^+ h^-$ *(h = π, K) decays and constraints on the CKM angle* γ, *Phys. Lett.* **B 718** (2012) 43 [arXiv:1209.5869] [INSPIRE].

[8] LHCb collaboration, *First observation of the decay* $\bar{B}_s^0 \to D^0 K^{*0}$ *and a measurement of the ratio of branching fractions* $\frac{\mathcal{B}(\bar{B}_s^0 \to D^0 K^{*0})}{\mathcal{B}(\bar{B}^0 \to D^0 \rho^0)}$, *Phys. Lett.* **B 706** (2011) 32 [arXiv:1110.3676] [INSPIRE].

[9] LHCb collaboration, *The LHCb Detector at the LHC*, 2008 *JINST* **3** S08005 [INSPIRE].

[10] R. Aaij et al., *The LHCb Trigger and its Performance*, arXiv:1211.3055 [INSPIRE].

[11] LHCb collaboration, R. Aaij et al., *Observation of $B^0 \to \overline{D}^0 K^+ K^-$ and evidence of $B_s^0 \to \overline{D}^0 K^+ K^-$*, *Phys. Rev. Lett.* **109** (2012) 131801 [`arXiv:1207.5991`] [InSPIRE].

[12] PARTICLE DATA GROUP collaboration, J. Beringer et al., *Review of Particle Physics (RPP)*, *Phys. Rev.* **D 86** (2012) 010001 [InSPIRE].

[13] T. Sjöstrand, S. Mrenna and P.Z. Skands, *PYTHIA 6.4 Physics and Manual*, *JHEP* **05** (2006) 026 [`hep-ph/0603175`] [InSPIRE].

[14] I. Belyaev et al., *Handling of the generation of primary events in* GAUSS*, the LHCb simulation framework*, *Nucl. Sci. Symp. Conf. Rec.* (2010) 1155.

[15] D. Lange, *The EvtGen particle decay simulation package*, *Nucl. Instrum. Meth.* **A 462** (2001) 152 [InSPIRE].

[16] GEANT4 collaboration, J. Allison et al., *Geant4 developments and applications*, *IEEE Trans. Nucl. Sci.* **53** (2006) 270

[17] GEANT4 collaboration, S. Agostinelli et al., *GEANT4: A Simulation toolkit*, *Nucl. Instrum. Meth.* **A 506** (2003) 250 [InSPIRE].

[18] M. Clemencic et al., *The LHCb simulation application,* GAUSS*: design, evolution and experience*, *J. Phys. Conf. Ser.* **331** (2011) 032023.

[19] K.S. Cranmer, *Kernel estimation in high-energy physics*, *Comput. Phys. Commun.* **136** (2001) 198 [`hep-ex/0011057`] [InSPIRE].

[20] LHCb collaboration, *First evidence of direct CP-violation in charmless two-body decays of Bs mesons*, *Phys. Rev. Lett.* **108** (2012) 201601 [`arXiv:1202.6251`] [InSPIRE].

[21] LHCb collaboration, *Letter of Intent for the LHCb Upgrade*, CERN-LHCC-2011-001.

[22] LHCb collaboration, *Framework TDR for the LHCb Upgrade: Technical Design Report*, CERN-LHCC-2012-007.

The LHCb collaboration

R. Aaij[38], C. Abellan Beteta[33,n], A. Adametz[11], B. Adeva[34], M. Adinolfi[43], C. Adrover[6],
A. Affolder[49], Z. Ajaltouni[5], J. Albrecht[35], F. Alessio[35], M. Alexander[48], S. Ali[38], G. Alkhazov[27],
P. Alvarez Cartelle[34], A.A. Alves Jr[22,35], S. Amato[2], Y. Amhis[7], L. Anderlini[17,f], J. Anderson[37],
R. Andreassen[57], R.B. Appleby[51], O. Aquines Gutierrez[10], F. Archilli[18], A. Artamonov [32],
M. Artuso[53], E. Aslanides[6], G. Auriemma[22,m], S. Bachmann[11], J.J. Back[45], C. Baesso[54],
V. Balagura[28], W. Baldini[16], R.J. Barlow[51], C. Barschel[35], S. Barsuk[7], W. Barter[44], A. Bates[48],
Th. Bauer[38], A. Bay[36], J. Beddow[48], I. Bediaga[1], S. Belogurov[28], K. Belous[32], I. Belyaev[28],
E. Ben-Haim[8], M. Benayoun[8], G. Bencivenni[18], S. Benson[47], J. Benton[43], A. Berezhnoy[29],
R. Bernet[37], M.-O. Bettler[44], M. van Beuzekom[38], A. Bien[11], S. Bifani[12], T. Bird[51], A. Bizzeti[17,h],
P.M. Bjørnstad[51], T. Blake[35], F. Blanc[36], C. Blanks[50], J. Blouw[11], S. Blusk[53], A. Bobrov[31],
V. Bocci[22], A. Bondar[31], N. Bondar[27], W. Bonivento[15], S. Borghi[51], A. Borgia[53],
T.J.V. Bowcock[49], E. Bowen[37], C. Bozzi[16], T. Brambach[9], J. van den Brand[39], J. Bressieux[36],
D. Brett[51], M. Britsch[10], T. Britton[53], N.H. Brook[43], H. Brown[49], A. Büchler-Germann[37],
I. Burducea[26], A. Bursche[37], J. Buytaert[35], S. Cadeddu[15], O. Callot[7], M. Calvi[20,j],
M. Calvo Gomez[33,n], A. Camboni[33], P. Campana[18,35], A. Carbone[14,c], G. Carboni[21,k],
R. Cardinale[19,i], A. Cardini[15], H. Carranza-Mejia[47], L. Carson[50], K. Carvalho Akiba[2], G. Casse[49],
M. Cattaneo[35], Ch. Cauet[9], M. Charles[52], Ph. Charpentier[35], P. Chen[3,36], N. Chiapolini[37],
M. Chrzaszcz [23], K. Ciba[35], X. Cid Vidal[34], G. Ciezarek[50], P.E.L. Clarke[47], M. Clemencic[35],
H.V. Cliff[44], J. Closier[35], C. Coca[26], V. Coco[38], J. Cogan[6], E. Cogneras[5], P. Collins[35],
A. Comerma-Montells[33], A. Contu[15], A. Cook[43], M. Coombes[43], G. Corti[35], B. Couturier[35],
G.A. Cowan[36], D. Craik[45], S. Cunliffe[50], R. Currie[47], C. D'Ambrosio[35], P. David[8], P.N.Y. David[38],
I. De Bonis[4], K. De Bruyn[38], S. De Capua[51], M. De Cian[37], J.M. De Miranda[1], L. De Paula[2],
W. De Silva[57], P. De Simone[18], D. Decamp[4], M. Deckenhoff[9], H. Degaudenzi[36,35], L. Del Buono[8],
C. Deplano[15], D. Derkach[14], O. Deschamps[5], F. Dettori[39], A. Di Canto[11], J. Dickens[44],
H. Dijkstra[35], P. Diniz Batista[1], M. Dogaru[26], F. Domingo Bonal[33,n], S. Donleavy[49], F. Dordei[11],
A. Dosil Suárez[34], D. Dossett[45], A. Dovbnya[40], F. Dupertuis[36], R. Dzhelyadin[32], A. Dziurda[23],
A. Dzyuba[27], S. Easo[46,35], U. Egede[50], V. Egorychev[28], S. Eidelman[31], D. van Eijk[38],
S. Eisenhardt[47], U. Eitschberger[9], R. Ekelhof[9], L. Eklund[48], I. El Rifai[5], Ch. Elsasser[37], D. Elsby[42],
A. Falabella[14,e], C. Färber[11], G. Fardell[47], C. Farinelli[38], S. Farry[12], V. Fave[36], D. Ferguson[47],
V. Fernandez Albor[34], F. Ferreira Rodrigues[1], M. Ferro-Luzzi[35], S. Filippov[30], C. Fitzpatrick[35],
M. Fontana[10], F. Fontanelli[19,i], R. Forty[35], O. Francisco[2], M. Frank[35], C. Frei[35], M. Frosini[17,f],
S. Furcas[20], E. Furfaro[21], A. Gallas Torreira[34], D. Galli[14,c], M. Gandelman[2], P. Gandini[52], Y. Gao[3],
J. Garofoli[53], P. Garosi[51], J. Garra Tico[44], L. Garrido[33], C. Gaspar[35], R. Gauld[52], E. Gersabeck[11],
M. Gersabeck[51], T. Gershon[45,35], Ph. Ghez[4], V. Gibson[44], V.V. Gligorov[35], C. Göbel[54],
D. Golubkov[28], A. Golutvin[50,28,35], A. Gomes[2], H. Gordon[52], M. Grabalosa Gándara[5],
R. Graciani Diaz[33], L.A. Granado Cardoso[35], E. Graugés[33], G. Graziani[17], A. Grecu[26],
E. Greening[52], S. Gregson[44], O. Grünberg[55], B. Gui[53], E. Gushchin[30], Yu. Guz[32], T. Gys[35],
C. Hadjivasiliou[53], G. Haefeli[36], C. Haen[35], S.C. Haines[44], S. Hall[50], T. Hampson[43],
S. Hansmann-Menzemer[11], N. Harnew[52], S.T. Harnew[43], J. Harrison[51], P.F. Harrison[45],
T. Hartmann[55], J. He[7], V. Heijne[38], K. Hennessy[49], P. Henrard[5], J.A. Hernando Morata[34],
E. van Herwijnen[35], E. Hicks[49], D. Hill[52], M. Hoballah[5], C. Hombach[51], P. Hopchev[4],
W. Hulsbergen[38], P. Hunt[52], T. Huse[49], N. Hussain[52], D. Hutchcroft[49], D. Hynds[48], V. Iakovenko[41],
P. Ilten[12], J. Imong[43], R. Jacobsson[35], A. Jaeger[11], E. Jans[38], F. Jansen[38], P. Jaton[36], F. Jing[3],
M. John[52], D. Johnson[52], C.R. Jones[44], B. Jost[35], M. Kaballo[9], S. Kandybei[40], M. Karacson[35],
T.M. Karbach[35], I.R. Kenyon[42], U. Kerzel[35], T. Ketel[39], A. Keune[36], B. Khanji[20], O. Kochebina[7],
I. Komarov[36,29], R.F. Koopman[39], P. Koppenburg[38], M. Korolev[29], A. Kozlinskiy[38], L. Kravchuk[30],

K. Kreplin[11], M. Kreps[45], G. Krocker[11], P. Krokovny[31], F. Kruse[9], M. Kucharczyk[20,23,j],
V. Kudryavtsev[31], T. Kvaratskheliya[28,35], V.N. La Thi[36], D. Lacarrere[35], G. Lafferty[51], A. Lai[15],
D. Lambert[47], R.W. Lambert[39], E. Lanciotti[35], G. Lanfranchi[18,35], C. Langenbruch[35], T. Latham[45],
C. Lazzeroni[42], R. Le Gac[6], J. van Leerdam[38], J.-P. Lees[4], R. Lefèvre[5], A. Leflat[29,35],
J. Lefrançois[7], O. Leroy[6], Y. Li[3], L. Li Gioi[5], M. Liles[49], R. Lindner[35], C. Linn[11], B. Liu[3], G. Liu[35],
J. von Loeben[20], J.H. Lopes[2], E. Lopez Asamar[33], N. Lopez-March[36], H. Lu[3], J. Luisier[36],
H. Luo[47], A. Mac Raighne[48], F. Machefert[7], I.V. Machikhiliyan[4,28], F. Maciuc[26], O. Maev[27,35],
S. Malde[52], G. Manca[15,d], G. Mancinelli[6], N. Mangiafave[44], U. Marconi[14], R. Märki[36], J. Marks[11],
G. Martellotti[22], A. Martens[8], L. Martin[52], A. Martín Sánchez[7], M. Martinelli[38],
D. Martinez Santos[39], D. Martins Tostes[2], A. Massafferri[1], R. Matev[35], Z. Mathe[35], C. Matteuzzi[20],
M. Matveev[27], E. Maurice[6], A. Mazurov[16,30,35,e], J. McCarthy[42], R. McNulty[12], B. Meadows[57,52],
F. Meier[9], M. Meissner[11], M. Merk[38], D.A. Milanes[13], M.-N. Minard[4], J. Molina Rodriguez[54],
S. Monteil[5], D. Moran[51], P. Morawski[23], J. Mountain[53], I. Mous[38], F. Muheim[47], K. Müller[37],
R. Muresan[26], B. Muryn[24], B. Muster[36], P. Naik[43], T. Nakada[36], R. Nandakumar[46], I. Nasteva[1],
M. Needham[47], N. Neufeld[35], A.D. Nguyen[36], T.D. Nguyen[36], C. Nguyen-Mau[36,o], M. Nicol[7],
V. Niess[5], R. Niet[9], N. Nikitin[29], T. Nikodem[11], S. Nisar[56], A. Nomerotski[52], A. Novoselov[32],
A. Oblakowska-Mucha[24], V. Obraztsov[32], S. Oggero[38], S. Ogilvy[48], O. Okhrimenko[41],
R. Oldeman[15,d,35], M. Orlandea[26], J.M. Otalora Goicochea[2], P. Owen[50], B.K. Pal[53], A. Palano[13,b],
M. Palutan[18], J. Panman[35], A. Papanestis[46], M. Pappagallo[48], C. Parkes[51], C.J. Parkinson[50],
G. Passaleva[17], G.D. Patel[49], M. Patel[50], G.N. Patrick[46], C. Patrignani[19,i], C. Pavel-Nicorescu[26],
A. Pazos Alvarez[34], A. Pellegrino[38], G. Penso[22,l], M. Pepe Altarelli[35], S. Perazzini[14,c],
D.L. Perego[20,j], E. Perez Trigo[34], A. Pérez-Calero Yzquierdo[33], P. Perret[5], M. Perrin-Terrin[6],
G. Pessina[20], K. Petridis[50], A. Petrolini[19,i], A. Phan[53], E. Picatoste Olloqui[33], B. Pietrzyk[4],
T. Pilař[45], D. Pinci[22], S. Playfer[47], M. Plo Casasus[34], F. Polci[8], G. Polok[23], A. Poluektov[45,31],
E. Polycarpo[2], D. Popov[10], B. Popovici[26], C. Potterat[33], A. Powell[52], J. Prisciandaro[36],
V. Pugatch[41], A. Puig Navarro[36], W. Qian[4], J.H. Rademacker[43], B. Rakotomiaramanana[36],
M.S. Rangel[2], I. Raniuk[40], N. Rauschmayr[35], G. Raven[39], S. Redford[52], M.M. Reid[45],
A.C. dos Reis[1], S. Ricciardi[46], A. Richards[50], K. Rinnert[49], V. Rives Molina[33], D.A. Roa Romero[5],
P. Robbe[7], E. Rodrigues[51], P. Rodriguez Perez[34], G.J. Rogers[44], S. Roiser[35], V. Romanovsky[32],
A. Romero Vidal[34], J. Rouvinet[36], T. Ruf[35], H. Ruiz[33], G. Sabatino[22,k], J.J. Saborido Silva[34],
N. Sagidova[27], P. Sail[48], B. Saitta[15,d], C. Salzmann[37], B. Sanmartin Sedes[34], M. Sannino[19,i],
R. Santacesaria[22], C. Santamarina Rios[34], E. Santovetti[21,k], M. Sapunov[6], A. Sarti[18,l],
C. Satriano[22,m], A. Satta[21], M. Savrie[16,e], D. Savrina[28,29], P. Schaack[50], M. Schiller[39],
H. Schindler[35], S. Schleich[9], M. Schlupp[9], M. Schmelling[10], B. Schmidt[35], O. Schneider[36],
A. Schopper[35], M.-H. Schune[7], R. Schwemmer[35], B. Sciascia[18], A. Sciubba[18,l], M. Seco[34],
A. Semennikov[28], K. Senderowska[24], I. Sepp[50], N. Serra[37], J. Serrano[6], P. Seyfert[11], M. Shapkin[32],
I. Shapoval[40,35], P. Shatalov[28], Y. Shcheglov[27], T. Shears[49,35], L. Shekhtman[31], O. Shevchenko[40],
V. Shevchenko[28], A. Shires[50], R. Silva Coutinho[45], T. Skwarnicki[53], N.A. Smith[49], E. Smith[52,46],
M. Smith[51], K. Sobczak[5], M.D. Sokoloff[57], F.J.P. Soler[48], F. Soomro[18,35], D. Souza[43],
B. Souza De Paula[2], B. Spaan[9], A. Sparkes[47], P. Spradlin[48], F. Stagni[35], S. Stahl[11],
O. Steinkamp[37], S. Stoica[26], S. Stone[53], B. Storaci[37], M. Straticiuc[26], U. Straumann[37],
V.K. Subbiah[35], S. Swientek[9], V. Syropoulos[39], M. Szczekowski[25], P. Szczypka[36,35], T. Szumlak[24],
S. T'Jampens[4], M. Teklishyn[7], E. Teodorescu[26], F. Teubert[35], C. Thomas[52], E. Thomas[35],
J. van Tilburg[11], V. Tisserand[4], M. Tobin[37], S. Tolk[39], D. Tonelli[35], S. Topp-Joergensen[52],
N. Torr[52], E. Tournefier[4,50], S. Tourneur[36], M.T. Tran[36], M. Tresch[37], A. Tsaregorodtsev[6],
P. Tsopelas[38], N. Tuning[38], M. Ubeda Garcia[35], A. Ukleja[25], D. Urner[51], U. Uwer[11], V. Vagnoni[14],
G. Valenti[14], R. Vazquez Gomez[33], P. Vazquez Regueiro[34], S. Vecchi[16], J.J. Velthuis[43], M. Veltri[17,g],
G. Veneziano[36], M. Vesterinen[35], B. Viaud[7], D. Vieira[2], X. Vilasis-Cardona[33,n], A. Vollhardt[37],

D. Volyanskyy[10], D. Voong[43], A. Vorobyev[27], V. Vorobyev[31], C. Voß[55], H. Voss[10], R. Waldi[55], R. Wallace[12], S. Wandernoth[11], J. Wang[53], D.R. Ward[44], N.K. Watson[42], A.D. Webber[51], D. Websdale[50], M. Whitehead[45], J. Wicht[35], J. Wiechczynski[23], D. Wiedner[11], L. Wiggers[38], G. Wilkinson[52], M.P. Williams[45,46], M. Williams[50,p], F.F. Wilson[46], J. Wishahi[9], M. Witek[23], W. Witzeling[35], S.A. Wotton[44], S. Wright[44], S. Wu[3], K. Wyllie[35], Y. Xie[47,35], F. Xing[52], Z. Xing[53], Z. Yang[3], R. Young[47], X. Yuan[3], O. Yushchenko[32], M. Zangoli[14], M. Zavertyaev[10,a], F. Zhang[3], L. Zhang[53], W.C. Zhang[12], Y. Zhang[3], A. Zhelezov[11], A. Zhokhov[28], L. Zhong[3], A. Zvyagin[35].

1   *Centro Brasileiro de Pesquisas Físicas (CBPF), Rio de Janeiro, Brazil*
2   *Universidade Federal do Rio de Janeiro (UFRJ), Rio de Janeiro, Brazil*
3   *Center for High Energy Physics, Tsinghua University, Beijing, China*
4   *LAPP, Université de Savoie, CNRS/IN2P3, Annecy-Le-Vieux, France*
5   *Clermont Université, Université Blaise Pascal, CNRS/IN2P3, LPC, Clermont-Ferrand, France*
6   *CPPM, Aix-Marseille Université, CNRS/IN2P3, Marseille, France*
7   *LAL, Université Paris-Sud, CNRS/IN2P3, Orsay, France*
8   *LPNHE, Université Pierre et Marie Curie, Université Paris Diderot, CNRS/IN2P3, Paris, France*
9   *Fakultät Physik, Technische Universität Dortmund, Dortmund, Germany*
10 *Max-Planck-Institut für Kernphysik (MPIK), Heidelberg, Germany*
11 *Physikalisches Institut, Ruprecht-Karls-Universität Heidelberg, Heidelberg, Germany*
12 *School of Physics, University College Dublin, Dublin, Ireland*
13 *Sezione INFN di Bari, Bari, Italy*
14 *Sezione INFN di Bologna, Bologna, Italy*
15 *Sezione INFN di Cagliari, Cagliari, Italy*
16 *Sezione INFN di Ferrara, Ferrara, Italy*
17 *Sezione INFN di Firenze, Firenze, Italy*
18 *Laboratori Nazionali dell'INFN di Frascati, Frascati, Italy*
19 *Sezione INFN di Genova, Genova, Italy*
20 *Sezione INFN di Milano Bicocca, Milano, Italy*
21 *Sezione INFN di Roma Tor Vergata, Roma, Italy*
22 *Sezione INFN di Roma La Sapienza, Roma, Italy*
23 *Henryk Niewodniczanski Institute of Nuclear Physics Polish Academy of Sciences, Kraków, Poland*
24 *AGH University of Science and Technology, Kraków, Poland*
25 *National Center for Nuclear Research (NCBJ), Warsaw, Poland*
26 *Horia Hulubei National Institute of Physics and Nuclear Engineering, Bucharest-Magurele, Romania*
27 *Petersburg Nuclear Physics Institute (PNPI), Gatchina, Russia*
28 *Institute of Theoretical and Experimental Physics (ITEP), Moscow, Russia*
29 *Institute of Nuclear Physics, Moscow State University (SINP MSU), Moscow, Russia*
30 *Institute for Nuclear Research of the Russian Academy of Sciences (INR RAN), Moscow, Russia*
31 *Budker Institute of Nuclear Physics (SB RAS) and Novosibirsk State University, Novosibirsk, Russia*
32 *Institute for High Energy Physics (IHEP), Protvino, Russia*
33 *Universitat de Barcelona, Barcelona, Spain*
34 *Universidad de Santiago de Compostela, Santiago de Compostela, Spain*
35 *European Organization for Nuclear Research (CERN), Geneva, Switzerland*
36 *Ecole Polytechnique Fédérale de Lausanne (EPFL), Lausanne, Switzerland*
37 *Physik-Institut, Universität Zürich, Zürich, Switzerland*
38 *Nikhef National Institute for Subatomic Physics, Amsterdam, The Netherlands*
39 *Nikhef National Institute for Subatomic Physics and VU University Amsterdam, Amsterdam, The Netherlands*
40 *NSC Kharkiv Institute of Physics and Technology (NSC KIPT), Kharkiv, Ukraine*
41 *Institute for Nuclear Research of the National Academy of Sciences (KINR), Kyiv, Ukraine*
42 *University of Birmingham, Birmingham, United Kingdom*
43 *H.H. Wills Physics Laboratory, University of Bristol, Bristol, United Kingdom*

44 *Cavendish Laboratory, University of Cambridge, Cambridge, United Kingdom*

45 *Department of Physics, University of Warwick, Coventry, United Kingdom*

46 *STFC Rutherford Appleton Laboratory, Didcot, United Kingdom*

47 *School of Physics and Astronomy, University of Edinburgh, Edinburgh, United Kingdom*

48 *School of Physics and Astronomy, University of Glasgow, Glasgow, United Kingdom*

49 *Oliver Lodge Laboratory, University of Liverpool, Liverpool, United Kingdom*

50 *Imperial College London, London, United Kingdom*

51 *School of Physics and Astronomy, University of Manchester, Manchester, United Kingdom*

52 *Department of Physics, University of Oxford, Oxford, United Kingdom*

53 *Syracuse University, Syracuse, NY, United States*

54 *Pontifícia Universidade Católica do Rio de Janeiro (PUC-Rio), Rio de Janeiro, Brazil, associated to* [2]

55 *Institut für Physik, Universität Rostock, Rostock, Germany, associated to* [11]

56 *Institute of Information Technology, COMSATS, Lahore, Pakistan, associated to* [53]

57 *University of Cincinnati, Cincinnati, OH, United States, associated to* [53]

[a] *P.N. Lebedev Physical Institute, Russian Academy of Science (LPI RAS), Moscow, Russia*

[b] *Università di Bari, Bari, Italy*

[c] *Università di Bologna, Bologna, Italy*

[d] *Università di Cagliari, Cagliari, Italy*

[e] *Università di Ferrara, Ferrara, Italy*

[f] *Università di Firenze, Firenze, Italy*

[g] *Università di Urbino, Urbino, Italy*

[h] *Università di Modena e Reggio Emilia, Modena, Italy*

[i] *Università di Genova, Genova, Italy*

[j] *Università di Milano Bicocca, Milano, Italy*

[k] *Università di Roma Tor Vergata, Roma, Italy*

[l] *Università di Roma La Sapienza, Roma, Italy*

[m] *Università della Basilicata, Potenza, Italy*

[n] *LIFAELS, La Salle, Universitat Ramon Llull, Barcelona, Spain*

[o] *Hanoi University of Science, Hanoi, Viet Nam*

[p] *Massachusetts Institute of Technology, Cambridge, MA, United States*